International Journal of Nanoelectronics and Materials
Volume 11, No. 1, Jan 2018 [25-32]

Electronic and Optical Properties of Ramsdellite TiO_2through mBJPotential

Jamal Sayah[1], Larbi El Farh[2,*], Hamza El Kouch[3] and Allal Challioui[4*]

[1,2,3]*Laboratory of Mechanic and Energetic, Faculty of Science, University Mohammed 1st Oujda, Morocco.*
[4]*Laboratory of Macromolecular Organic Chemistry and Natural Products, Faculty of Science, University Mohammed 1stOujda, Morocco.*

Received 30 May 2017; Revised 7 July 2017; Accepted 19 July 2017

ABSTRACT

The aim of this work is to study the electronic and optical properties of ramsdellite titanium dioxide (TiO_2), using the first principle calculations with modified Becke-Johnson (mBJ) exchange potential. By comparison with the experimental data done by other reseachers, the obtained results allowed us to conclude that the calculated electronic properties with the mBJ approximation are significantly improved than those obtained using others methods such as Generalized Gradient Approximation (GGA) and the Local Density Approximation (LDA).Thus, a gap of 3.4 eV with mBJ, which is very close to the value 3.34 eV was found by experimental work. The optical parameters such as the dielectric constant, refractive index, extinction coefficient, reflectivity, optical conductivity and energy loss were also calculated.

Keywords: Ramsdellite TiO_2, Electronic Properties, Optical Properties, FP–LAPW, LDA, GGA,TB-mBJ.

1. INTRODUCTION

Several modern technologies use titanium dioxide (TiO_2) as a base material because of its point defects [1-9] such as solar cells [10] and Li-ion batteries. Furthermore, TiO_2 has a rich phase diagram comprising many polymorphs: rutile, anatase, brookite, bronze, hollandite, ramsdellite, cotunnite, fluorite, pyrite [11-12]. The majority of studies focused on three crystalline phases (anatase, rutile and brookite). For example, Tran and Blaha's modified the Becke–Johnson (TB-mBJ) exchange potential [17-18] method within the Density Functional Theory (DFT) which has already been proven in the study of electronic structures and optical properties of rutile and anatase TiO_2 [19]. Moreover, in recent years, some experimental studies [14-16] have been focusing on the use of TiO_2 ramsdellite as electrode in the electrochemical energy storage in Li-Ion batteries. Despite that, this work is the first to investigate the electronic structures and optical properties of ramsdellite TiO_2(R).This study focused on ramsdellite polymorph of titanium dioxide, TiO_2 (R), having TiO_6-octahedra less regular [13].

The comparative calculations with experimental data show that the mBJ energy gaps are substantially improved than LDA and GGA values [20]. Besides that, the optical properties for

*Corresponding author: Jamal Sayah , Larbi El Farh, Hamza ElKouch, AllalChallioui,
Laboratory of Mechanic and Energetic, Faculty of Science, University Mohammed 1stOujda, Morocco.
Laboratory of Macromolecular Organic Chemistry and Natural Products, Faculty of Science, University Mohammed 1stOujda, Morocco.

ramsdellite TiO_2 such as the dielectric functions, refractive index, extinction coefficient, reflectivity coefficients, conductivity and the energy-loss spectrum were also calculated and discussed.

2. COMPUTATION DETAILS

In this work, DFT calculations [21-22] with Tran and Blaha-modified Becke–Johnson potential (TB-mBJ) are applied to obtain the electronic band structure and the density of states (DOS) for ramsdellite TiO_2 (R) compound. WIEN2k computer package [23] was used to implemented the full potential (FP) linearized-augmented plane wave (LAPW) plus local orbital (LO) (FP/LAPW+LO). The electronic band gap obtained by this method is closer to the experimental value compared to electronic band gap obtained by LDA or GGA.

The product (RMT*Kmax) equal to 8 was taken since this value is found as the optimal value for energy convergence, where the RMT is Muffin-Tin sphere radii and Kmax is the cut-off wave vector in the first Brillouin zone. In this calculations, RMT(Ti) = 2.0 a.u. and RMT(O) = 1.50 a.u were taken and the integration in Brillouin zone was made with 3000 k-points.

The convergence of the self-consistent calculations was considered as reached only when the integration of absolute charge-density difference per formula unit between the successive loops is less than 0.0001e, where e is the electron charge.

3. ELECTRONIC STRUCTURE

3.1 Structural

Figure 1 shows orthorhombic structure of ramsdellite TiO_2, with Pbnm symmetry. It consists of TiO_6-octahedra.The lattice parameters and atoms coordinates for ramsdellite TiO_2 obtained through calculation and experimental measurement were provided in Table 1 and 2 respectively.

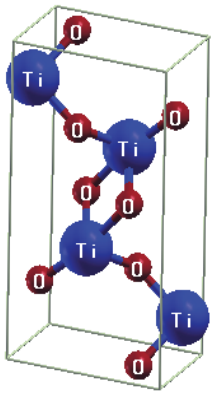

Figure 1. Structure of ramsdellite TiO_2

Table 1 Lattice parameters of ramsdellite TiO_2

Lattice parameters(Å)	Calculation	Experiment [24]
A	4.95	4.90
B	9.58	9.46
C	2.97	2.96

Table 2 Atoms coordinates in ramsdellite TiO_2

Atom	Calculation			Experiment [25]		
	X	y	z	x	y	z
Ti	-0.081	0.183	0.25	-0.77	0.135	0.25
O1	0.638	0.268	0.25	0.636	0.206	0.25
O2	0.202	-0.032	0.25	0.238	-0.222	0.25

3.2 Band Structures

Figure 2 shows the calculated energy band structures of ramsdellite TiO_2 with LDA, GGA and TB-mBJ. In the three cases, the maximum of the valence band (VBM) and minimum of the conduction band is at the Γ point. This indicates a direct band gap (ΓC -ΓV) with the following values: 2.4 eV for LDA, 2.8 eV for GGA and 3.4 eV for mBJ. Takahashi et al. [20] measured the Ultraviolet-Visible absorption of ramsdellite TiO_2 and found band gap energy of 3.34 eV.

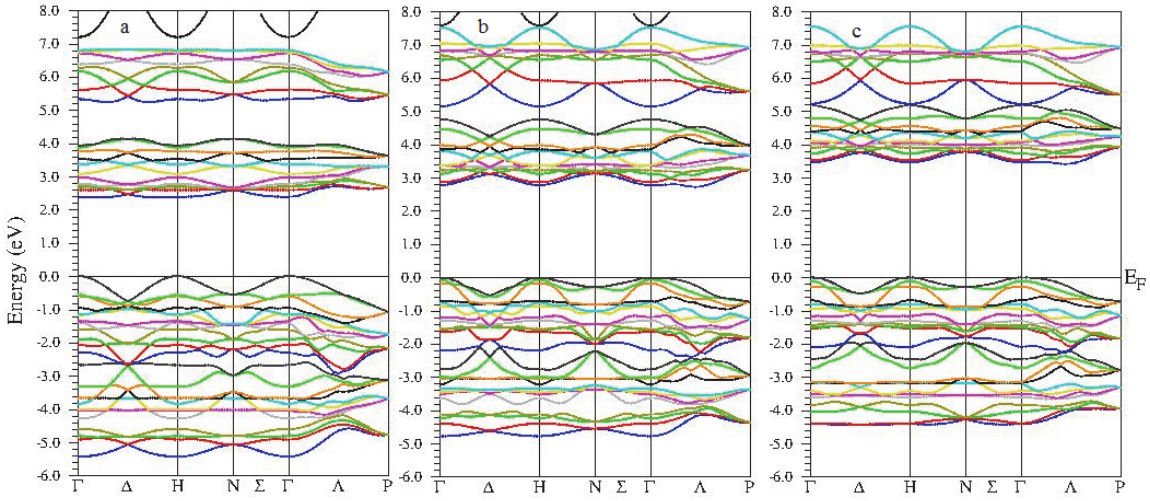

Figure 2. Calculated band structures of TiO_2 (R) with (a) LDA, (b) GGA and(c) mBJ methods

The calculated and experimental band gaps values are summarized in Table 3. These results show that the value of the energy band gap obtained by mBJ approach is very close to the experimental value [20] compared tothe values obtained by LDA or GGA.

Table 3 Calculated and experimental values of bands gaps of ramsdellite TiO_2

Method	LDA	GGA	mBJ	Exp [20]
Band Gaps (eV)	2.4	2.8	3.4	3.34

3.3 Electronic Properties

Figure 3 shown the total calculated density of states (DOS) and atomic orbitals of ramsdellite TiO_2 (R) obtained using mBJ. There are four bands in the DOS observed. The first left band located at

about −4 eV is principally due to O 2p states with a small contribution from Ti 3d states. The next band centered at about -1.5 eV is mainly due to O 2p states. Above the Fermi level, the bands located at about 4 eV and 7 eV are principally due to Ti 3d states with small contribution from O 2p states.

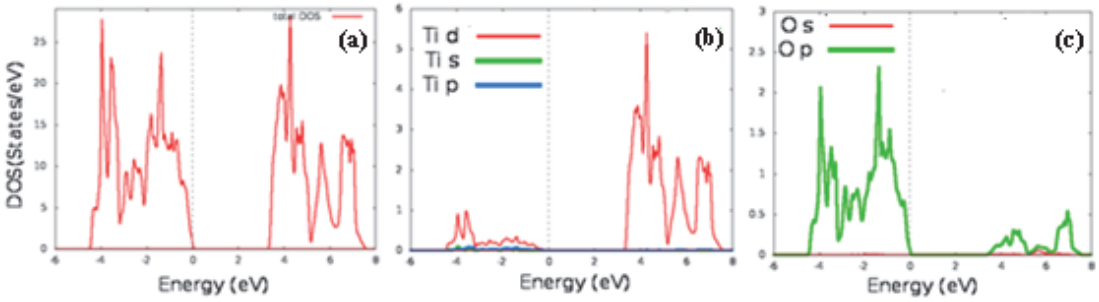

Figure 3. DOS (a) total and (b) partial Ti and (c) partial O using TB-mBJ for ramsdellite TiO_2

4. OPTICAL PROPERTIES

4.1 Optical dielectric functions

The dielectric function is given by Eq. (1), where $\varepsilon_2(\omega)$ describe the absorptive behavior and $\varepsilon_1(\omega)$ gives information about the electronic polarizability of material that can be extracted from $\varepsilon_2(\omega)$ using the Kramers-Kronig relation [26].

$$\varepsilon(\omega) = \varepsilon_1(\omega) + i\varepsilon_2(\omega) \qquad (1)$$

The real and imaginary parts, respectively $\varepsilon_1(\omega)$ and $\varepsilon_2(\omega)$, of the dielectric function are represented in Figure 4 respectively for E//a (4a) and E//c (4b), within the photon energy window of 0–12 eV. $\varepsilon_1(\omega)$ begin by increasing until a maximum value at 3.7 eV for E//a and 3.9 eV for E//c and then goes down to negative values between about 7.5 and 12 eV for both E//a and E//c. $\varepsilon_1(\omega)$ negative implies that the material is reflective.The static dielectric constant at zero frequency, $\varepsilon^a(0)$ for E//a and $\varepsilon^c(0)$ for E//c, are presented in Table 4, using mBJ method.

Table 4 Calculated static dielectric constant at zero frequency for TiO_2 (R) using TB-mBJ

	mBJ method
$\varepsilon^a(0)$	4
$\varepsilon^c(0)$	5.2

The edge of the optical absorption in ramsdellite TiO_2 (R) occurs at about 3.2 eV [27]. In this Γ point (ΓV– ΓC) occurs splitting between valence and conduction bands, and it is the direct gap of optical transition between the highest valence band and the lowest conduction band. This study suggests that this compound has a strong absorption region extended between 3.6 eV and 9 eV, and beyond this region, three important peak scan be seen. The first peak located at around 3.5 eV and 4.5 eV respectively for E//a and E//c is due to the electronic transition from O 2p states of the valence band (VB) to Ti 3d and O 2p states in conduction band (CB). The second peak situated at 5.3 eV and 6.2 eV respectively for E//a and E//c is due to the inter-band transitions between O 2p valence states and O 2s, p, Ti 3d conduction states. The peak

situated at 7.3 eV and at 7.6 eV respectively for E//a and E//c originates from direct optical transitions between O 2p and Ti 2p valence states and O s, p and Ti d, s conduction band.

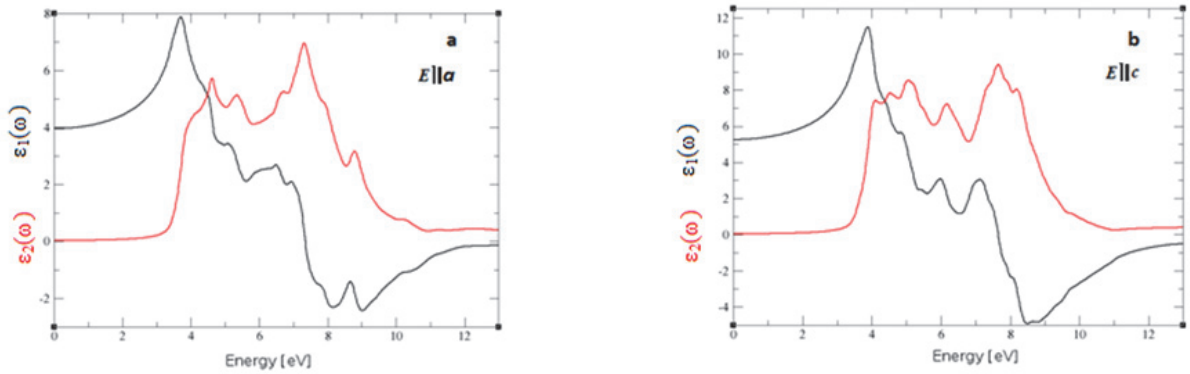

Figure 4. Real (ε_1) (black) and imaginary (ε_2) (red) parts of dielectric functions versus photon energy (eV) of ramsdellite TiO_2 respectively for (a) E ‖ a and (b) E ‖ c

4.2 Refractive index n(ω)and extinction coefficient k(ω)

The values of the real and imaginary parts of the frequency dependent dielectric function provide basis for the calculation of the refractive index n(ω) [28]. The refractive index n(ω) are displayed in Figure 5(a) for E//a (black) and E//c (red). The refractive index is almost constant until 1 eV, after which it increases with energy until a maximum value of 2.8 for E//a and 3.5 for E//C at around 3.8 eV.

In Figure 5(b), the extinction coefficients, k(ω) for E//a (black) and E//c (red), that was determined theoretically was sketched out. Some similarities were highlighted between the behavior of k(ω) and n(ω). Figure 5(b) shows the first peak of roughly k(ω) = 1.75 at about 5 eV for E//c, and k (ω) = 1.2 at around 4.6 eV for E//a. This first peak is followed by several other ones that appear to be quantitatively more present for E//c comparing with E//a, and with higher intensities as well.

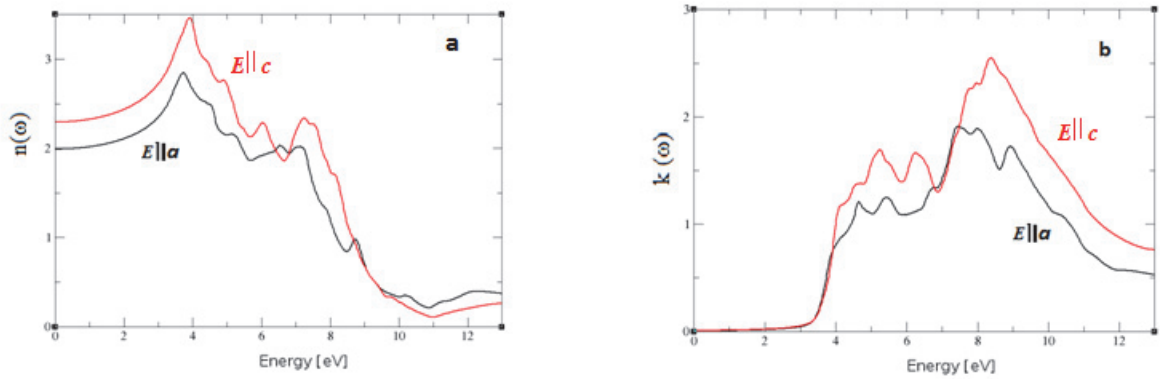

Figure 5. (a) Refractive indexes n(ω) for E//a (black) and E//c (red) and (b) extinction coefficient k(ω) for E//a (black) and E//c (red) versus photon energy (eV) of ramsdellite TiO_2

4.3 Reflectivity R(ω)

The optical reflectivity R(ω) is displayed in Figure 6 and the zero-frequency reflectivity is 11% and 16% respectively for E//a and E//c. The maximum reflectivity value is about 58.3% at 9.6 eV and 84.2% at 10.9 eV respectively for E//a and E//c. Figure 4(a) and Figure 6 show that when the real part of dielectric function $\varepsilon_1(\omega)$ is negative, we get the maximum reflectivity.

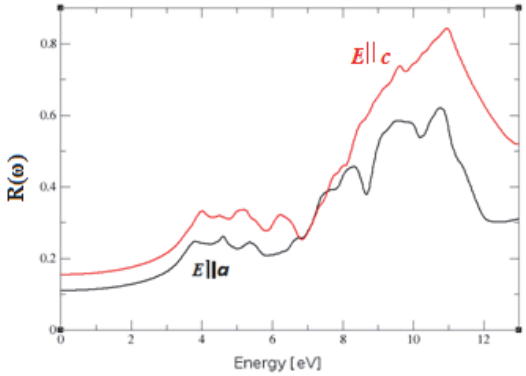

Figure 6. Reflectivity R(ω) of ramsdellite TiO_2 for E ‖ a (black) and E ‖ c (red)

4.4 Optical conductivity σ(ω)

The optical conductivity is given by Eq. (2). The real part $\sigma_1(\omega)$ of optical conductivity is shown by black curves in Figure 7(a) for E//a and Figure 7(b) for E//c. The two curves are almost constant up to about 3 eV. Then, the first curve shows a maximum value of optical conductivity at about 7.3 eV with a magnitude of 615200 $\Omega^{-1}cm^{-1}$. As for the second curve, the maximum is at about 7.7 eV with a magnitude of 871300 $\Omega^{-1}cm^{-1}$.

$$\sigma(\omega) = \sigma_1(\omega) + i\,\sigma_2(\omega) \tag{2}$$

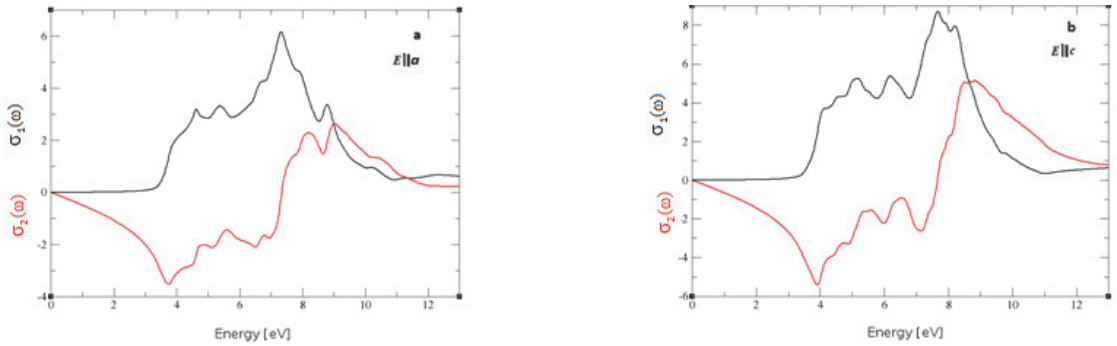

Figure 7. Real part (black curve) and imaginary part (red curve) of optical conductivity functions versus photon energy (eV) of TiO_2 (R), (a) for E//a and (b) for E//c

The imaginary part $\sigma_2(\omega)$ of optical conductivity is shown by red curves in Figure 7a for E//a and Figure 7(b) for E//c. It starts decreasing below 0 in negative scale for the ranges of 0 and 7.3 eV for the first curve and the ranges of 0 and 7.7 eV for the second curve. The compound has a maximum value of optical conductivity at about 9 eV with a magnitude of 264400 $\Omega^{-1}.cm^{-1}$for E//a and 514800 $\Omega^{-1}.cm^{-1}$ for E//c.

4.5 The energy-loss spectrum L(ω)

Figure 8 shows energy loss function L(ω). This function allows describing the energy loss of a fast photon traversing a material. The peaks appearing in these spectra are associated with the plasma resonance. It is at about 13.2 eV for E//a, and about 13.1 eV for E//c.

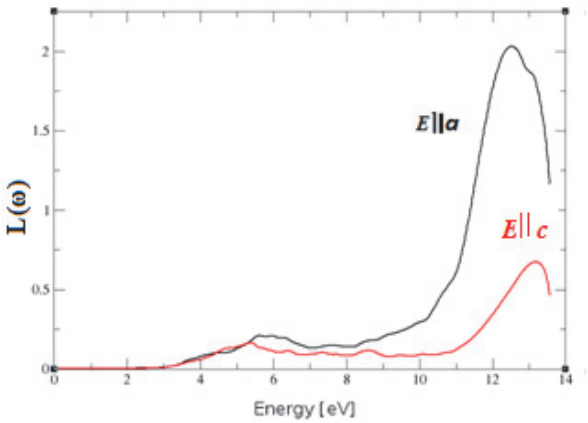

Figure 8. Energy-loss spectrum L(ω) of ramsdellite TiO_2 (black curve) for E//a and (red curve) E//c

5. CONCLUSION

Firstly, the electronic properties of the ramsdellite TiO_2(R) were studied using density functional theory with approximations namely GGA, LDA and the modified Becke–Johnson mBJ exchange potential as implemented in WIEN2k code. This study shows that the use of mBJ gives a gap of 3.4 eV, which the closest to the experimental value of 3.34 eV found by Takahashi et al. [20] while that values found by the LDA and GGA approximations were relatively lower, 2.4 eV and 2.8 eV respectively.

From total and partial DOS calculated for ramsdellite TiO_2(R) obtained using mBJ, it can be seen that there are four bands in the DOS, two in the valance band due principally to O 2p states and two others in the conduction band due principally to Ti 3d states.
The optical study of ramsdellite TiO_2, using mBJ, indicated three electronic transition 1) from O 2p states of the valence band (VB) to Ti 3d and O 2p states in conduction band (CB), 2) inter-band between O 2p valence states and O 2s, p, Ti 3d conduction states and 3) direct optical between O 2p and Ti 2p valence states and O s, p and Ti d, s conduction band.

The refractive index n(ω) and the extinction coefficient k(ω) shows some similarities. Noted that, when the real part of dielectric function $\varepsilon_1(\omega)$ is negative, the reflectivity is maximum. The real part $\sigma_1(\omega)$ of optical conductivity is almost constant up to about 3 eV. Then, a maximum value appear at about 7.5 eV with a magnitude 1.5 times greater for E//c than for E//a.

The imaginary part $\sigma_2(\omega)$ of optical conductivity shows a maximum value at about 9 eV with a magnitude of 2 times greater for E//c than for E//a. Moreover, the peak in the spectra of energy loss function L(ω) is associated with the plasma resonance.

REFERENCES

[1] V. Swamy, J. D. Galeb, L. S. Dubrovinsky, Journal of Physics and Chemistry of Solids **62** (2001) 887.
[2] A. N. Banerjee, Journal Nanostructures Nanotechnology Science and Applications **4** (2011) 35.
[3] K. Noami, Y. Muraoka, T. Wakita, M. Hirai, Y. Kato, T. Muro, Y. Tamenori, T. Yokoya, Journal of Applied Physics **107** (2010) 073910.
[4] Z. Yang, D. Choi, S. Kerisit, K. M. Rosso, D. Wang, J. Zhang, G. Graff, J. Liu, A review Journal of Power Sources **192** (2009) 588.

[5] B. Prasai, B. Cai, M. K. Underwood, J. P. Lewis, D. A. Drabold, Journal of Materials Science **47** (2012) 7515.
[6] M. Stamate, G. Lazar, I. Lazar, Romanian Journal of Physics **53** (2008) 217.
[7] M. Kobayashi, H. Kato, M. Kakihana, Journal Nanomaterials and Nanotechnology **3** (2013) 1.
[8] Y. Xiaohui,L. Changsheng, L. Yun, T. Ting-Ao, W. Qiong, K. Junjie, Computational Materials Science **49** (2010) 430.
[9] L. Chunxia, D. Suihu, Z. Caili, W. Liping, H. Peide, Optik - International Journal for Light and Electron Optics **125** (2014) 3145.
[10] M. Devi, Manas R. Panigrahi, Int. J. Nanoelectronics and Materials **10**(2017) 63.
[11] Q. Jun Liu, Z. Ran, F. Sheng Liu, Z. Tang Liu, Journal of Alloys and Compounds **631** (2015) 192.
[12] Z. Tong, P. G. Shang, The Journal of Physical Chemistry **118** (2014) 11385.
[13] M. V. Koudriachova, Chemical Physics Letters **458** (2008) 108.
[14] R. K. B. Gover, J. R. T Tolchard, H. Tukamoto, T. Murai, J. T. S. Irvine, J. Electrochem. Soc. **146** (1999) 4348.
[15] A. Kuhn, R. Amandi, F. García-Alvarado, J. Power Sources **92**(2001) 221.
[16] J. C. Pérez-Flores, M. Hoelzel, F. García-Alvarado, A. Kuhn, Chem. Phys. Chem. **17** (2016) 1062.
[17] D. Koller, F. Tran, P. Blaha, Physical Rewiew B**85** (2012) 15109.
[18] F. Tran, P. Blaha, Physical Review Letters **102** (2009) 226401.
[19] Gong Sai, Liu Bang-Gui, Chin. Phys. B **21**(2012) 057104.
[20] I. Y. Takahash, N. Kijima, J. Akimoto, Chemistry of Materials **18** (2006) 784.
[21] W. Kohn, L. J. Sham, Physical Review **140** (1965) 1133.
[22] P. Hohenberg, W. Kohn, Physical Review **136** (1964) 864.
[23] B. Peter, S. Karlheinz, M. Georg, K. Dieter, L. Joachim,WIEN2K11.1 (2011) 7-11.
[24] J. Akimoto, Y. Gotoh, Y. Osawa, T. Kumagai, K. Aoki, Journal of Solid State Chemistry **113** (1994) 27.
[25] A. Kuhn, C. Baehtz, F. Garcıa-Alvarado, Journal of Power Sources **174** (2007) 421.
[26] B. Amin, R. Khenata, A. Bouhemadou, A. Iftikhar, M. Maqbool, Physica B: Condensed Matter **407** (2012) 2588.
[27] A.M. Shehap, Dana S. Akil, Int. J. Nanoelectronics and Materials **9**(2016) 17.
[28] G. Murtaza, A. Iftikhar, B. Amin, A. Afaq, M. Maqbool, J. Maqsood, I. Khan, M. Zahid,. Optical Materials **33** (2011) 553.